Light-Induced Structural Changes in the LOV2 Domain of *Adiantum* Phytochrome3 Studied by Low-Temperature FTIR and UV−Visible Spectroscopy†

Tatsuya Iwata,[‡,§] Dai Nozaki,[§] Satoru Tokutomi,[‡] Takatoshi Kagawa,[||,⊥,#] Masamitsu Wada,[⊥,@] and Hideki Kandori*[,§]

Research Institute for Advanced Science and Technology, University of Osaka Prefecture, Sakai, Osaka 599-8570, Japan, Department of Applied Chemistry, Nagoya Institute of Technology, Showa-ku, Nagoya 466-8555, Japan, PRESTO (Precursory Research for Embryonic Science and Technology), Japan Science and Technology Corporation, 1-8 Honcho 4-chome, Kawaguchi, Saitama 332-0012, Japan, Division of Biological Regulation and Photobiology, National Institute for Basic Biology, Okazaki 444-8585, Japan, and Department of Biological Sciences, Graduate School of Science, Tokyo Metropolitan University, Tokyo 192-0397, Japan

Received April 1, 2003; Revised Manuscript Received May 2, 2003

ABSTRACT: Phototropin (Phot) is a blue-light receptor in plants. The molecule has two FMN (flavin mononucleotide) binding domains named LOV (light-, oxygen-, and voltage-sensing), which is a subset of the PAS (Per-Arnt-Sim) superfamily. Illumination of the phot-LOV domains in the dark state (D447) produces a covalent C(4a) flavin−cysteinyl adduct (S390) via a triplet excited state (L660), which reverts to D447 in the dark. In this work, we studied the light-induced structural changes in the LOV2 domain of *Adiantum* phytochrome3 (phy3), which is a fusion protein of phot containing the phytochrome chromophoric domain, by low-temperature UV−visible and FTIR spectroscopy. UV−visible spectroscopy detected only one intermediate state, S390, in the temperature range from 77 to 295 K, indicating that the adduct is produced even at temperatures as low as 77 K, although a portion of D447 cannot be converted to S390 at low temperatures possibly because of motional freezing. In the whole temperature range, FTIR spectra in the S−H stretching frequency region showed that Cys966 of phy3-LOV2 is protonated in D447 and unprotonated on illumination, supporting adduct formation. The pK_a of the S−H group in D447 is estimated to be >10. FTIR spectra also showed the light-induced appearance of a positive peak around 3621 cm^{-1} in the whole temperature range, indicating that adduct formation accompanies rearrangement of a hydrogen bond of a water molecule(s), which can be either water25, water45, or both, near the chromophore. In contrast to the weak temperature dependence of the spectral changes in the UV−visible absorption and the FTIR of both S−H and O−H stretching bands, light-induced changes in the amide I vibration that probes protein backbone structure vary significantly with the increase in temperature. The spectral changes suggest that light excitation of FMN loosens the local structure around it, particularly in turns, in the early stages and that another change subsequently takes place to tighten it, mainly in β-structure, but some occur in the α-helical structure of the protein moiety as well. Interestingly, these changes proceed without altering the shape of UV−visible spectra, suggesting the presence of multiple conformation states in S390.

Plants use visible light as a signal from their environments and as an energy source for photosynthesis. Plants sense red/far-red and blue light by phytochrome and blue-light receptors (*1*), respectively. One of the major blue-light receptors, phototropin (phot), regulates phototropic response (*2*), relocation of chloroplast (*3*), and opening of stomata (*4*), which are deeply involved in improving the efficiency of photosynthesis. Higher plants have two isoforms of phot, phot1 and phot2, that share these responses *via* their different sensitivities to light (*5*). In addition to phot1 and phot2, *Adiantum* has a fusion protein of phot in its C-terminus with a chromophoric domain of phytochrome in its N-terminus, which is named phytochrome3 (phy3) (*6*) and acts as a red-light sensor for *Adiantum* in its survival in the canopy of forests (*7*).

Phototropins are composed of ∼1000 amino acid residues and two prosthetic FMN[1] molecules. The N-terminal half has two chromophoric domains binding FMN molecules noncovalently, and the C-terminal half has Ser/Thr kinase motifs. The two chromophoric domains (ca. 100 residues) are named LOV1 and -2, since they have primary (*8*) and tertiary (*9*) structures highly homologous to those of the LOV

† This work was supported in part by grants from the Japanese Ministry of Education, Culture, Sports, Science, and Technology (Grant 13139205 to S.T. and Grant 14658215 to H.K.), and by the NITECH 21st Century COE Program to T.I.

* To whom correspondence should be addressed. Phone & Fax: 81-52-735-5207. E-mail: kandori@ach.nitech.ac.jp.

‡ University of Osaka Prefecture.

§ Nagoya Institute of Technology.

|| Japan Science and Technology Corp.

⊥ National Institute for Basic Biology.

Present address: Institute for Applied Biochemistry, University of Tsukuba, Tsukuba 305-8572, Japan.

@ Tokyo Metropolitan University.

[1] Abbreviations: FMN, flavin mononucleotide; LOV, light-, oxygen-, and voltage-sensing; PAS, Per-Arnt-Sim; FTIR, Fourier transform infrared; UV, ultraviolet.

10.1021/bi0345135 CCC: $25.00
Published on Web 06/17/2003

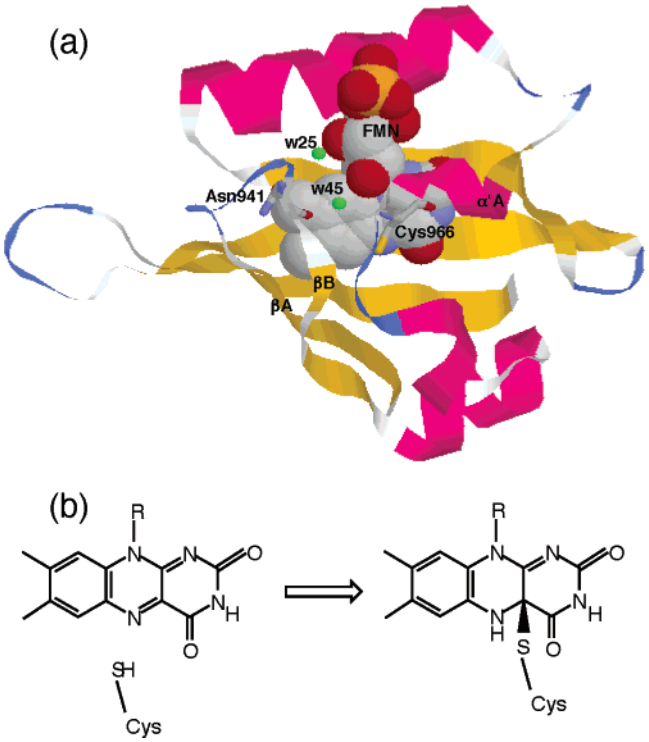

FIGURE 1: (a) Protein structure of phy3-LOV2 (PDB entry 1G28) (*9*). The whole structure is shown as a ribbon drawing, where helices, turns, and sheets are colored red, blue, and yellow, respectively. FMN is shown as a space-filling drawing, while Cys966 and Asn941 are shown as stick drawings. FMN binds LOV2 noncovalently, and Cys966 is located at the N-terminal side of helix α′A. Two water molecules (water25 and water45) near FMN are shown as green balls. The folding motif of this protein is characteristic of the LOV domain, which belongs to the PAS superfamily. (b) Photoreaction scheme for the phototropin LOV domains. Cysteine is protonated in the initial state, and forms an adduct with FMN upon light absorption.

(light-, oxygen-, and voltage-sensing) domain, which is a subset of the PAS (Per-Arnt-Sim) superfamily (Figure 1a). Light enhances autophosphorylation of phot molecules both *in vivo* and *in vitro* (*10*, *11*). Although the involvement of the autophosphorylation in signal transduction and the presence of a substrate(s) for the kinase activity have not been shown, photon energy absorbed by the FMN regulates the kinase activity through unknown molecular processes occurring in both the chromophore and the protein moieties.

It is well-known that *cis*−*trans* photoisomerization of the chromophore initiates chain reactions of light-signal transduction in most of the photoreceptors studied so far, such as rhodopsin (*12*), phytochrome (*13*), and photoactive yellow protein (PYP) (*14*). Photoisomerization alters chromophore structure and induces structural changes in the protein moiety, followed by specific protein−protein interactions that activate the transducer protein. However, this is not the case for phot since FMN has no isomerizable double bonds. To elucidate the primary photoreaction of phot, its two photoactive LOV domains have been expressed and used for spectroscopic analyses. Illumination of the phot-LOV domain causes a loss of yellow color, forming a product absorbing at ∼390 nm (S390), which reverts to the ground state in the dark (*15*). Since the spectrum of S390 resembles that of a covalent C(4a) flavin−cysteinyl adduct (*16*), formation of a flavin−cysteinyl adduct in the LOV domain has been suggested. Several experiments such as mutation of the cysteine (*15*, *17*), NMR spectroscopy (*18*), and X-ray crystallography of S390 (*19*) have provided experimental evidence that favors formation of the adduct in S390.

By measuring time-resolved absorption spectra of oat phot1-LOV2, Swartz et al. have shown that there are only two photocycle intermediates, L660 and S390, the former of which was proposed to be an excited triplet state (*17*). Very recently, a radical-pair mechanism was proposed for this FMN−C(4a)-cysteinyl adduct formation based on ESR studies (*20*). Swartz et al. have also proposed that the cysteinyl group is deprotonated in the ground state (*17*). To stabilize the thiolate, they postulated the presence of a counter charge, an XH^+ group. We have recently shown that the cysteine (Cys966) of phy3-LOV2 is in the protonated S−H form, not in thiolate, on the basis of the infrared spectral analysis (Figure 1b) (*21*). Upon formation of S390, the S−H stretch disappears, presumably forming the adduct between FMN and Cys966. This observation is consistent with the crystal structure of phy3-LOV2 (*19*), which contained no amino acids suitable for serving as the XH^+ group near Cys966 surrounded by hydrophobic amino acids. Our observation is also consistent with the FTIR results obtained recently for *Chlamydomonas* phot-LOV1 (*22*).

The results obtained so far indicate that S390 is the only intermediate in the electronic ground state, which is formed from L660 with a time constant of 4 μs in oat phot2-LOV2 (*17*) and with constants of 900 ns and 4 μs in *Chlamydomonas* phot-LOV1 (*23*). This is in contrast to other photoreceptive proteins with photoisomerizable chromophores described above. In visual rhodopsin, for instance, the primary intermediate is formed on a time scale of femtoseconds, followed by the sequential appearance of other intermediates in pico-, nano-, micro-, and milliseconds (*12*), which is evident from changes in their UV−vis absorption spectra. Furthermore, X-ray crystallography of photolyzed species, S390, of *Adiantum* phy3-LOV2 revealed a protein structure very similar to that of the ground state, D447. This is also in contrast to the photoreceptors with isomerizable chromophores since their photoreactions are accompanied by marked structural changes in their protein moieties (*12*−*14*). Similarly, small structural changes during photoreception were reported from crystallographic studies of PYP (*24*) that has a photoisomerizable chromophore and is a member of the LOV domain family. However, it was claimed that larger structural changes can be observed in solutions than in crystals, and that the small changes are due to the structural constraints in crystals (*25*−*28*). Then, the question of whether the reported small structural changes of phy3-LOV2 are characteristic for flavin-type photoreceptors or due to the fact that the observation was made in a crystal arises.

In this work, we studied light-induced structural changes in *Adiantum* phy3-LOV2 by low-temperature UV−visible and FTIR spectroscopy. Spectral changes in the UV−visible and wide midinfrared region were monitored at 77−295 K. We observed only one intermediate, S390, in this temperature range from UV−visible spectroscopy. This is consistent with the previous report of oat phot1-LOV2 and *Chlamydomonas* phot-LOV1 by time-resolved UV−visible spectroscopy (*17*, *23*). S390 formation is accompanied by the disappearance of an S−H stretching vibration. In contrast, the amide I vibration that probes protein structure varies significantly over the range of measurement temperatures. These results

strongly suggest that phy3-LOV2 has progressive structural changes in the protein moiety like other photoreceptive proteins, which happen without a change in the UV−visible absorption. The FTIR spectra also detected structural changes involving a water(s) near the FMN during the photoconversion to S390. The mechanism of these light-induced structural changes in phy3-LOV2 is discussed.

MATERIALS AND METHODS

Sample Preparation. A fusion protein of the LOV2 domain of *Adiantum* phytochrome3 (phy3) (*29*) with calmodulin-binding peptide (CBP) was prepared by using the pCAL-n-EK affinity protein expression and purification system (Stratagene). The construct containing N-terminal CBP and spanning amino acid residues 905−1087 of phy3 was expressed in *Escherichia coli* BL21(DE3) pLysS cells (Novagen). A large-scale culture was grown at 37 °C to an OD_{600} of 0.3−0.4. Expression was performed in darkness for 4 h at 28 °C in the presence of 0.5 mM isopropyl β-D-galactopyranoside. The overexpressed fusion protein was purified by a calmodulin resin column under a dim red safety light according to the instructions. The eluate containing CBP-bound phy3-LOV2 was dialyzed against 1 mM potassium phosphate buffer (pH 7) or borate buffer (pH 10), and then concentrated to give a final concentration of 2.1 mg/mL as determined with a Microcon YM-10 instrument (Millipore). Concentrations were determined on the basis of a reported extinction coefficient of 11 200 M^{-1} cm^{-1} at 450 nm for *Adiantum* phy3-LOV2 (*6*). Ninety microliters of the solution was placed on a BaF_2 window, and then dried to a film under reduced pressure with an aspirator. The films were hydrated as follows. A drop of either H_2O or $H_2{}^{18}O$ was put next to the film on the window, which was sealed with the second window and a rubber ring, and then left for 2 h at room temperature to ensure full hydration. The hydrated films are stable as judged from their spectral integrity after storage for a few months at 4 °C.

Spectroscopy. UV−visible and infrared spectra of the hydrated films were measured using V-550DS (JASCO) and FTS-7000 (Bio-Rad) spectrophotometers, respectively. Low-temperature spectra were measured by using a cryostat (Optistat DN, Oxford) and a temperature controller (ITC 4, Oxford) with liquid nitrogen as the coolant. The data are presented as difference spectra between after and before the illumination of the sample with >400 nm light for 1 min, which was supplied with a combination of a halogen−tungsten lamp (250 W) and a long-pass filter (L42, Toshiba) and was proven to be sufficient to saturate the photoconversion of the samples (*21*). For FTIR spectra, 128 interferograms at 2 cm^{-1} resolution were recorded before and after illumination, and 8−10 recordings were averaged.

RESULTS

Low-Temperature UV−Visible Spectra of Phy3-LOV2. Figure 2 shows light *minus* dark difference UV−visible spectra of phy3-LOV2 (pH 7) measured at temperatures from liquid nitrogen to ambient. All the spectra look similar, possessing negative peaks at 268, 449, and 475 nm as well as a positive peak at 304 nm. They also have a small peak at ~400 nm, and a broad negative feature in the wavelength region of 330−390 nm. These results reproduced our earlier

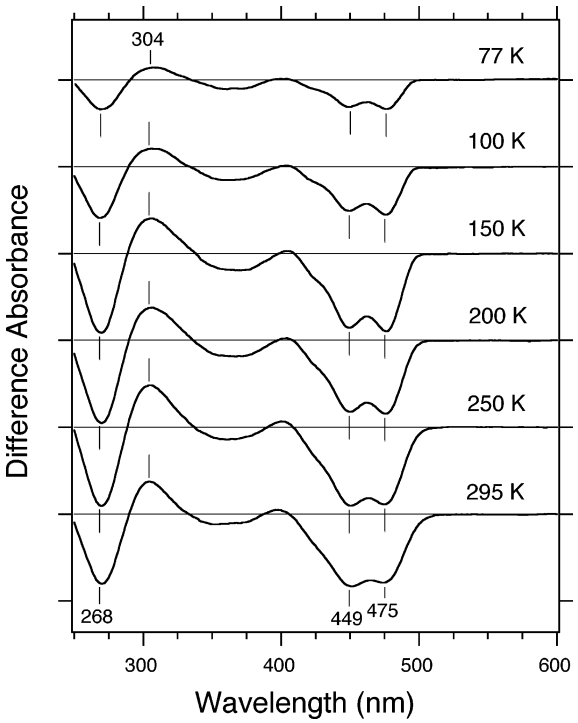

FIGURE 2: Light *minus* dark difference spectra for phy3-LOV2 (pH 7) in the UV−visible region. The spectra were recorded at 77, 100, 150, 200, 250, and 295 K. One division of the *y*-axis corresponds to 0.03 absorbance unit.

ones measured at 150 and 295 K (*21*). They are characteristic spectra of the S390 *minus* ground state, D447 (*17*), indicating that S390 is formed at all the temperatures that were used. It should be noted that absorption spectra of D447 (without illumination) were temperature-dependent, and the peak at 475 nm is sharpened at low temperatures. Consequently, the negative features in the 400−500 nm region in Figure 2 differ at various temperatures. Since S390 was stable at every temperature except 295 K, we warmed the sample to room temperature for reversion of S390 to D447 for each UV−vis and FTIR measurement.

Interestingly, the obtained amplitudes of the difference spectra were smaller at 77 and 100 K. The peak amplitudes at 77 and 100 K are 36 and 64%, respectively, of those at the other temperatures. Neither prolonged illumination by >400 nm nor illuminations by the other wavelengths increased the amplitudes at 77 and 100 K, indicating that the smaller amplitudes cannot be ascribed to insufficient illumination at these temperatures. There are two possible explanations for the smaller amplitudes. (1) The extinction coefficient of S390 (or both D447 and S390) is smaller, and (2) some fraction of phy3-LOV2 molecules cannot convert to S390 and remain in the D447 at these low temperatures. Since the absolute absorption spectra showed complete photoconversion of D447 to S390 at the higher temperatures, and the absorption peak around 450 nm remained even after prolonged illumination at low temperatures, the second explanation is the case.

Low-Temperature FTIR Spectra of Phy3-LOV2 in the 1600−950 cm^{-1} Region. Figure 3 shows light *minus* dark difference IR spectra in the 1600−950 cm^{-1} region measured at temperatures from liquid nitrogen to ambient. The IR spectra were similar to each other, possessing positive bands at 1542, 1430, 1374, 1302, 1259, and 1094 cm^{-1} and negative

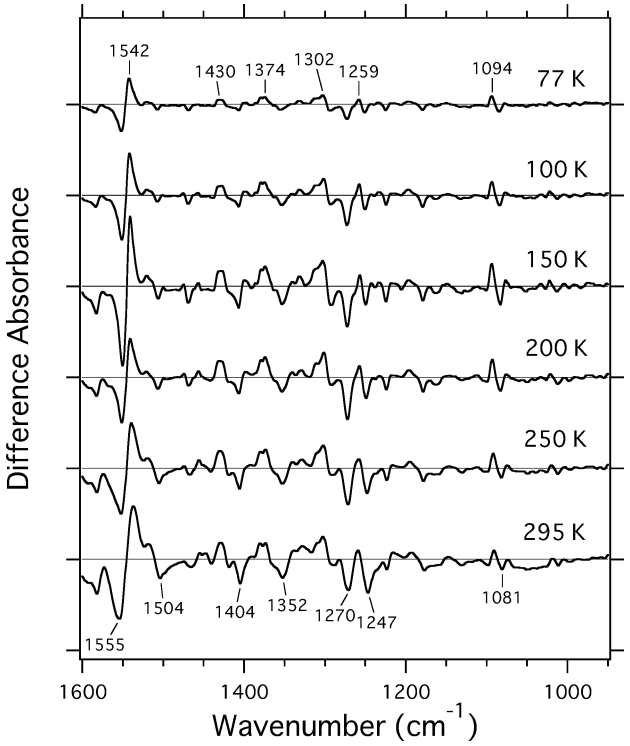

FIGURE 3: Light *minus* dark infrared difference spectra for phy3-LOV2 (pH 7) in the 1600−950 cm^{-1} region. The spectra were recorded at 77, 100, 150, 200, 250, and 295 K. One division of the *y*-axis corresponds to 0.004 absorbance unit.

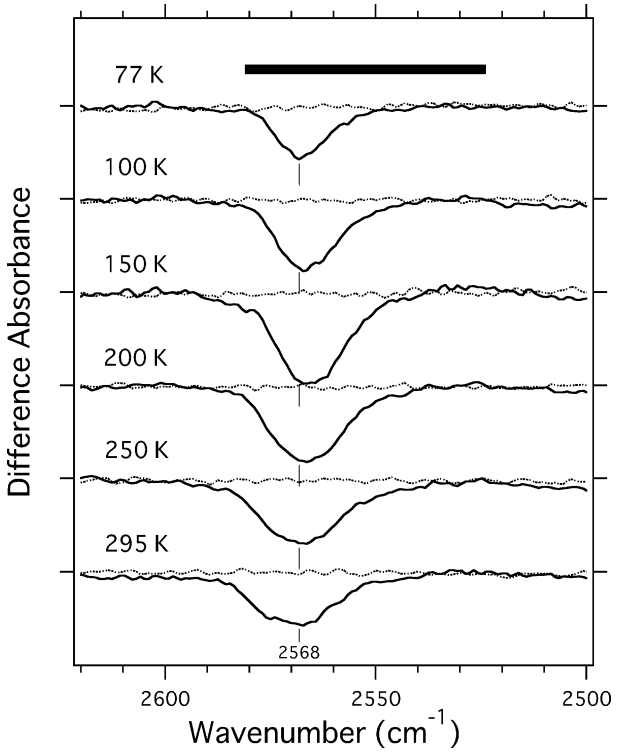

FIGURE 4: Light *minus* dark (solid line) and dark *minus* dark (dotted line) infrared difference spectra for phy3-LOV2 (pH 7) in the 2620−2500 cm^{-1} region. The spectra were recorded at 77, 100, 150, 200, 250, and 295 K. One division of the *y*-axis corresponds to 0.00012 absorbance unit. Thick horizontal bar (2580−2525 cm^{-1}) shows the frequency region of the S−H stretch known from the literature (*38*).

bands at 1555, 1504, 1404, 1352, 1270, and 1247 cm^{-1} (Figure 3). As for the UV−visible absorption spectra, the signal amplitudes of most bands were smaller at 77 and 100 K than those at the higher temperatures. Some bands, however, exhibited a different dependence on temperature. The negative 1555 cm^{-1} and positive 1542 cm^{-1} bands have a maximal amplitude at 150 K. Similar temperature dependence was observed for the positive 1094 cm^{-1} and negative 1081 cm^{-1} bands. Furthermore, the amplitude ratio of the marked band at 1270 cm^{-1} to that at 1247 cm^{-1} decreased with the increase in temperature. The reported resonance Raman data and normal mode calculation with oat phot1-LOV2 suggested that most of these bands originate from FMN, i.e., the chromophore of LOV2 (*30*).

Low-Temperature FTIR Spectra of Phy3-LOV2 in the S−H Stretching Region. Figure 4 shows difference IR spectra in the 2620−2500 cm^{-1} region measured at temperatures from liquid nitrogen to ambient. As we have reported previously (*21*), a negative band appears around 2568 cm^{-1} in the light *minus* dark spectrum (thick solid line), which is absent in the baseline (dotted line). The result clearly demonstrates the presence of S−H groups in D447 and their disappearance upon conversion to S390 (*21*). Since phy3-LOV2 has only one cysteine, the S−H stretching vibration comes from Cys966. The absence of respective positive bands is consistent with adduct formation of the S−H group with FMN. The negative band appeared in accordance with the formation of S390 at all the temperatures that were used from 77 to 295 K (compare Figures 2 and 4), confirming that adduct formation is coupled with photoconversion to S390.

S−H stretching vibrations appear in the 2580−2525 cm^{-1} region (thick bar in Figure 4), and their frequencies decrease as the hydrogen bonding of the S−H groups become stronger. The frequency of 2568 cm^{-1}, therefore, indicates that the S−H group is weakly hydrogen bonded in D447. This is consistent with the local structure around Cys966 of the Phy3-LOV2 crystal in the D447 state (*9*), where there are no amino acid residues or water molecules available to serve as the hydrogen bonding acceptor. Peak frequencies, which are estimated by spectral fitting with Gaussian functions, change by ∼3 cm^{-1} between the different temperatures: 2567 cm^{-1} at 77 K, 2566 cm^{-1} at 100, 150, and 200 K, 2567 cm^{-1} at 250 K, and 2569 cm^{-1} at 295 K. The peaks of the S−H stretch become broadened at higher temperatures, with spectral half-widths of 15 cm^{-1} at 77 K, 17 cm^{-1} at 100 K, 19 cm^{-1} at 150 K, 20 cm^{-1} at 200 K, and 22 cm^{-1} at 250 and 295 K. The significant broadening of the line width and the minor changes in the peak position indicate that the temperature increase from 77 to 295 K enhances the fluctuations in the microenvironment of the S−H bond of D447, but hardly affects the mode of the vibration.

Apparently, the peak amplitudes of the S−H bands are smaller at 77 and 100 K than at the higher temperatures, and seem to be maximal at 150 K, similar to the peaks at 1542 (+)/1555 (−) cm^{-1} and 1094 (+)/1081 (−)cm^{-1} (Figure 3). The amplitudes at 77 and 100 K can be calibrated by use of the observed UV−vis difference spectra (Figure 2), which showed that the fractions of D447 photoconverted to S390 at 77 and 100 K are 36 and 64%, respectively, of those at the higher temperatures. The peak heights normalized to the 100% population of S390 at 77 and 100 K are 2.1 and 1.8 times larger, respectively, than that at 295 K. If the effect of line broadening is taken into account, the calculated

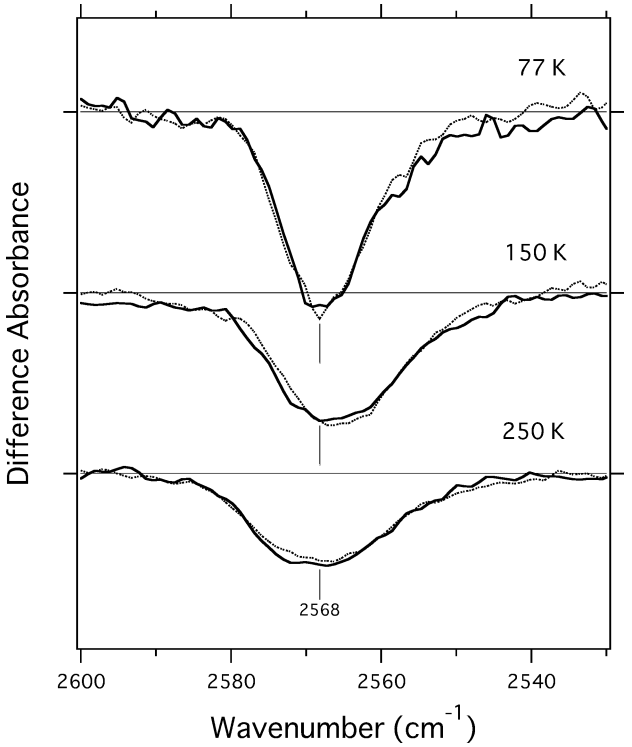

FIGURE 5: Light *minus* dark infrared difference spectra for phy3-LOV2 at pH 7 (dotted line) and pH 10 (solid line) in the 2620−2530 cm^{-1} region. The spectra were recorded at 77, 150, and 250 K. Note that the spectra at 77 K were divided by 0.36 so that the amount of D447 converted to S390 becomes the same. One division of the *y*-axis corresponds to 0.0002 absorbance unit.

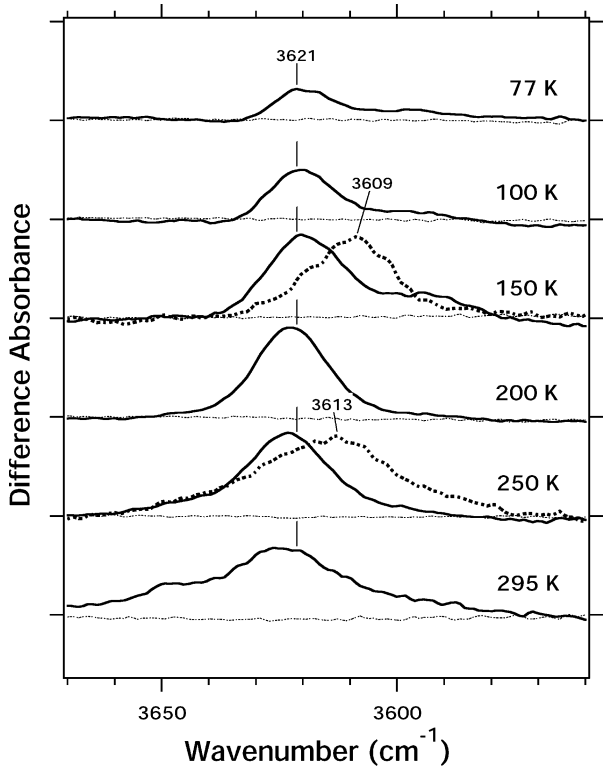

FIGURE 6: Light *minus* dark (solid line) and dark *minus* dark (thin dotted line) infrared difference spectra for phy3-LOV2 (pH 7) in the 3670−3560 cm^{-1} region. The spectra were recorded at 77, 100, 150, 200, 250, and 295 K. Thick dotted lines at 150 and 250 K represent the samples hydrated with $H_2{}^{18}O$. One division of the *y*-axis corresponds to 0.0005 absorbance unit.

areas of the S−H band become 1.65 and 1.56 times larger at 77 and 100 K, respectively.

There may be two origins for the larger negative bands at the lower temperatures: (i) the pK_a of the S−H group is temperature-dependent, and some fraction is not in the S−H form at the higher temperatures, or (ii) the absorption coefficient of the S−H stretch is larger at the lower temperatures. The first possibility was examined by measuring the magnitude of the negative S−H band at a neutral (*7*) and an alkaline (*10*) pH at 77, 150, and 250 K (Figure 5),[2] where the amplitude of the difference spectra at 77 K was normalized by use of UV−visible absorption. Since FMN is known to dissociate from LOV domains at acidic pH (*18*), the effect of acidic pH was not measured. The spectra in Figure 5 are almost superimposable between the two pHs at all the temperatures that were used. Thus, the protonation state of the S−H group is affected by neither the temperature between 77 and 250 K nor the pH between pH 7 and 10. The pK of cysteine in solution is reported to be 8.3−8.8, whereas the pK_a of the S−H group is estimated to be larger than 10. This is in line with the report that the adduct formation of oat phot1-LOV2 exhibited a minimal pH dependence between pH 3.7 and 9.5 (*31*). The higher pK_a of the SH in the LOV domain may be due to microenvironments around the cysteine in the chromophore pocket of the LOV2 domains. The observation excludes the first of the two alternatives.

Low-Temperature FTIR Spectra of Phy3-LOV2 in the Water O−H Stretching Region. Phy3-LOV2 has two internal water molecules, water25 and -45, within 5 Å of the FMN (Figure 1a). Since these water molecules are expected to be involved in formation of the adduct between Cys966 and FMN, IR spectra were measured in the O−H stretch regions. Figure 6 shows difference IR spectra in the 3670−3560 cm^{-1} region, the frequencies of which are characteristic of the O−H stretches of weakly hydrogen bonded waters (*32*). A prominent positive band appears around 3621 cm^{-1} in the light *minus* dark spectrum (thick solid line), which is absent in the dark *minus* dark spectrum (baseline, dotted line). In addition to the main band, a sideband appeared in the 3610−3580 cm^{-1} region at 77, 100, and 150 K. A different sideband appeared in the 3660−3640 cm^{-1} region at 250 and 295 K. There is no sideband at 200 K. The effect of H_2O substitution with $H_2{}^{18}O$ was measured at 150 and 250 K, where the 3621 cm^{-1} band shifted downward (Figure 6, thick dotted line); however, the sidebands did not shift. This indicates that the main positive band comes from the O−H stretch of an internal water molecule(s). The origins of the sidebands are as yet unknown.

Only positive peaks were observable in the >3560 cm^{-1} region for the light *minus* dark spectrum, suggesting that the corresponding negative peaks are present at a lower frequency for strongly hydrogen bonded O−H residues and undetectable due to the strong O−H vibrations from waters. Since the frequency of 3621 cm^{-1} implicates the O−H

[2] In this study, we made films from the sample solution at pH 7.0 or 10.0, and the pH of the hydrated films could not be exactly determined. However, our studies have shown that this method can adequately control the pH of the samples in the case of rhodopsins such as bacteriorhodopsin (*39*), visual rhodopsin (*40*), and *pharaonis* phoborhodopsin (*41*). It is also the case for PYP (H. Kandori, unpublished observation).

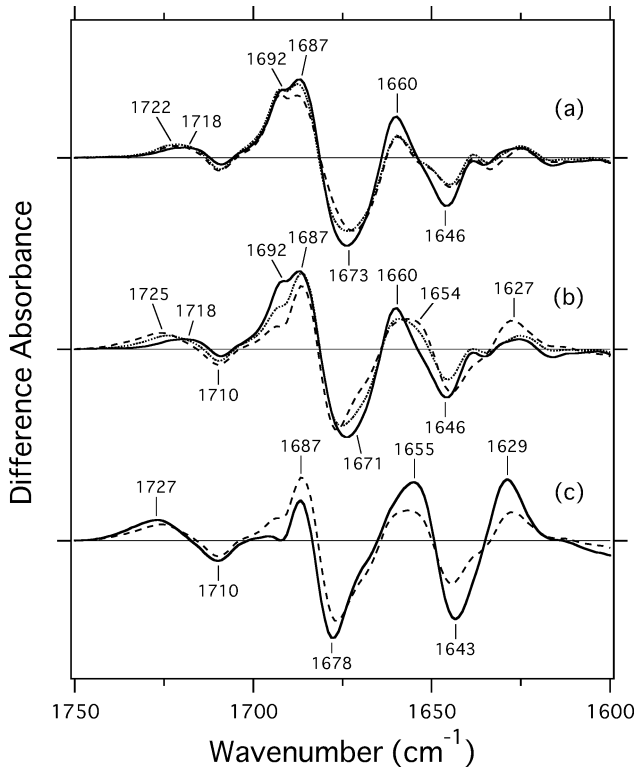

FIGURE 7: Light *minus* dark infrared difference spectra for phy3-LOV2 (pH 7) in the 1750−1600 cm^{-1} region. The spectra were recorded at 77 K (dashed line in part a), 100 K (dotted line in part a), 150 K (solid lines in parts a and b), 200 K (dotted line in part b), 250 K (dashed lines in parts b and c), and 295 K (thick solid line in part c). Note that the spectra at 77 and 100 K were divided by 0.36 and 0.64, respectively, so that the amount of D447 converted to S390 becomes the same at all the temperatures. One division of the *y*-axis corresponds to 0.0005 absorbance unit.

residues as being very weakly hydrogen bonded (*32*), the appearance of the positive 3621 cm^{-1} band shows the breakage of the hydrogen bond of the water molecule(s) during formation of the adduct between Cys966 and FMN. Since the band appears at even 77 K, the water molecule(s) involved in the adduct formation is probably located in the vicinity of the chromophore. Either water25, water45, or both, therefore, are the candidates for this (Figure 1a). X-ray crystallography revealed no positional shift of either water upon adduct formation (*19*). Nevertheless, breakage of hydrogen bonds of these molecules may be possible because of the motion of a hydrogen bonding acceptor.

Low-Temperature FTIR Spectra of Phy3-LOV2 in the Amide I Region. Figure 7 shows light *minus* dark difference IR spectra in the 1750−1600 cm^{-1} region. The spectra at 77 and 100 K are enlarged by 1/0.36 and 1/0.64, respectively, to normalize the population of D447 photoconverted to S390 to those at the higher temperatures as described above, and were used for the following analyses. The difference IR spectra show several bands in this region that obviously varied depending on temperature. This frequency region is known to be characteristic of amide I vibration that probes the C═O stretch of peptide backbone; however, it should be noted that vibrations of the chromophore, FMN, are present in this region also.

Vibrational bands in the 1730−1700 cm^{-1} region have been reported to be attributable to the symmetric C═O stretch of FMN in both oat phot1-LOV2 (*30*) and *Chlamydomonas* phot-LOV1 (*22*). In phy3-LOV2, the intensity of the minor negative peak at 1710 cm^{-1} at 77 K decreased slightly to have a minimal intensity at 150 K and then increased with a temperature up to 295 K. Its corresponding positive peak at 1722 cm^{-1} at 77 K shifted slightly to the lower frequency to have a minimal frequency at 150 K and then shifted to the higher frequency up to 1727 cm^{-1} from 150 to 295 K. Similar temperature dependencies with a break point at 150 K are observed in two pairs of bands, 1555/1542 and 1094/1081 cm^{-1}, that have been suggested to come from FMN (*30*), as described above. Accordingly, the bands observed with phy3-LOV2 in this region may result from the light-induced structural changes in FMN that depend on temperature with a discontinuity at 150 K.

On the other hand, vibration bands at 1700−1600 cm^{-1} can be ascribed to both FMN and amide I. In fact, symmetric and asymmetric C═O stretches and the C═C stretch of FMN in *Chlamydomonas* phot-LOV1 appear at ∼1710, ∼1670, and ∼1640 cm^{-1}, respectively (*22*). On the basis of the FTIR and Raman spectra, Ataka et al. argued that most of the vibrational changes in this region originate from those of FMN modes upon S390 formation in *Chlamydomonas* phot-LOV1 (*22*). In contrast, Swartz et al. reported the contribution of amide I vibrations to this region from their FTIR and Raman spectra of oat phot1-LOV2 (*30*). In phot-LOV1, the amplitude of the bands in the 1700−1600 cm^{-1} region, e.g., 1684 (+)/1672 (−) cm^{-1}, does not exceed 200% of the amplitude of the band at 1724 (+)/1712 cm^{-1} which is ascribed to FMN (*22*). On the other hand, phot1-LOV2 exhibited an amplitude of the band at 1686 (+)/1675 (−) cm^{-1} ∼5 times larger than that at 1725 (+)/1711 (−) cm^{-1} (*30*). Similarly, phy3-LOV2 in the study presented here exhibited 4−10 times larger bands in this region than at 1727 (+)/1710 (−) cm^{-1} (Figure 7a−c). These results suggest significant contributions of light-induced changes in amide I to the observed difference vibration bands of LOV2, being in contrast to those of LOV1. Amide I vibrations at 1700−1670 cm^{-1}, around 1655 cm^{-1}, and at 1640−1610 cm^{-1} have been shown to be characteristic of turn, helical, and β-sheet structures, respectively (*33*). The observed bands in Figure 7 in this region, at least partly, reflect the changes in these secondary structures of LOV2. Actually, a recent far-UV CD study on oat phot1-LOV2 suggests reversible loss of α-helicity during the photocycle (*31*).

The spectrum at 77 K has positive peaks at 1692, 1687, and 1660 cm^{-1} and negative peaks at 1673 and 1646 cm^{-1} (dashed line in Figure 7a). The spectral shape is not changed much at 100 K, except for a slight increase at 1687 cm^{-1} (dotted line in Figure 7a). The peaks at 1692 (+), 1687 (+), and 1673 (−) cm^{-1} can be attributed to the amide I vibrations of turn structure, and the bands at 1660 (+) and 1646 (−) cm^{-1} belong to those of a helical structure. Since the former is 4.9 times larger in intensity than the latter, structural changes of the peptide backbone at 77 and 100 K may take place mostly in turn structure. The peptide backbone of α-helix changes as well. Both the turn and helix peaks shifted to higher frequencies on phototransformation to S390, implying that hydrogen bonding of the peptide C═O groups is weakened by adduct formation. As the temperature is increased from 100 to 150 K, the pairs of the α-helical peaks at 1660 (+)/1646 (−) cm^{-1} and the turn peaks at 1687 (+)/1673 (−) cm^{-1} become larger (solid line in Figure 7a),

indicating that the extent of these changes increases at 150 K.

When the temperature is increased from 150 to 250 K, the difference spectra change more markedly. The positive peak at 1692 cm^{-1}, which has an almost constant amplitude below 150 K, decreases progressively at 200 K (dotted line in Figure 7b) and 250 K (dashed line in Figure 7b). Similarly, the negative peak at 1671−1673 cm^{-1}, the magnitude of which increases between 100 and 150 K, decreases between 150 and 250 K (Figure 7b). Since the bands at 1700−1670 cm^{-1} are attributable to the amide I vibrations of turn structure, these data imply that the hydrogen bonding networks of turn structure loosened upon adduct formation are retightened at the higher temperatures. Similarly, the magnitudes of the amide I vibrations from helical structure at 1660 (+) and 1646 (−) cm^{-1}, which increased between 100 and 150 K, decreased slightly at 200 K (dotted line in Figure 7b), suggesting that unfolded α-helix partially refolds again. In addition, a pair of new bands at 1654 (+)/1646 (−) cm^{-1} appears at 250 K. Thus, illumination seems to make the turn structure loose at the temperatures up to 150 K, which is accompanied by loosening of an α-helix and reverts partly between 150 and 250 K.

The other prominent spectral feature at 250 K is an appearance of the positive 1627 cm^{-1} band (compare the dashed lines in parts b and c of Figure 7), which is ascribed to the amide I vibrations of β-sheet. Its intensity becomes almost 2 times larger at 295 K with a slight peak shift to 1629 cm^{-1}, and is larger than that of the 1687 cm^{-1} band ascribed to the turn structure. In addition, the positive peak at 1692 cm^{-1} disappeared at 295 K. These observations suggest that structural changes of the peptide backbone at 295 K take place mainly in β-sheet structure, and those in turn structure are smaller than they were at the lower temperatures. The corresponding negative peaks of the bands at 1629 cm^{-1} (at 295 K) and 1627 cm^{-1} (at 250 K) are probably at 1643 and 1646 cm^{-1}, respectively, indicating shifts to lower frequencies. Therefore, the light-induced structural changes at these temperatures are suggested to tighten the hydrogen bond network in the β-structure. In addition, the 1654 cm^{-1} positive peak at 250 K almost doubled its intensity at 295 K with a slight peak shift to 1655 cm^{-1}, which also implies contributions from α-helical regions to the light-induced structural changes at 295 K.

DISCUSSION

We studied light-induced structural changes in the LOV2 domain of *Adiantum* phytochrome3 using low-temperature FTIR and UV−visible absorption spectroscopy. Only one photointermediate in the electronic ground state, S390, was detected in the temperature range from liquid nitrogen to ambient. This is consistent with the previous reports on oat phot1-LOV2 (*17*) and *Chlamydomonas* phot-LOV1 (*23*) from nanosecond time-resolved UV−visible spectroscopy at ambient temperatures. S390 can be formed at all the temperatures that were used, but only 36 and 64% of the total population of D447 can be converted to S390 at 77 and 100 K, respectively.

The incomplete conversion to S390 at these low temperatures is presumably due to freezing of molecular motions around FMN. The conformation of phy3-LOV2 in the D447 state must fluctuate in solution at ambient temperatures, where the distance between the cystein S−H group and C(4a) of FMN is changing rapidly. The distance of 4.2 Å in the crystal structure (*9*) represents the most stable state in that crystal. Enhanced dynamical motions at the higher temperatures enable phy3-LOV2 to form the cysteinyl−flavin adduct. However, reduced levels of molecular motion at 77 and 100 K may hinder the adduct formation.[3] A study, which is now in progress, on the temperature dependence of the quantum yield of the adduct formation will make this clear.

We have recently reported that Cys966 is protonated in the D447 state of *Adiantum* phy3-LOV2 (*21*), which is in contrast to the proposal for oat phot1-LOV2 (*17*). This study reproduced the previous observation of the S−H stretch in D447 at 77−295 K (Figure 4). Quantitative comparison among the temperatures, nevertheless, raises a possibility that the S−H group is partially deprotonated in D447 at the higher temperatures, since the area of the negative band at 77 and 100 K, calibrated by the fraction of formed S390, was 1.65 and 1.56 times, respectively, greater than that at 295 K. However, the possibility can be excluded because of the pH independence of the intensity as described in the Results. Instead, enhanced absorption of the S−H stretch in the D447 state at low temperatures is suggested, the reason for which is unclear. The protonated state of cysteine in D447 at ambient temperature is also supported by the FTIR observations in *Chlamydomonas* phot-LOV1 (*20*).

The FTIR study presented here revealed that the light-induced formation of the cysteinyl−flavin adduct is accompanied by structural changes in a water molecule(s) (Figure 6), which is possibly water25, water45, or both. The changes result in loosening of its (their) hydrogen bond network. It has been well established that rearrangements of hydrogen bond networks of internal water molecules are involved in photoinduced transformations of chromoproteins such as bacteriorhodopsin (*31*) and photoactive yellow protein (*26*). Adduct formation, therefore, may affect hydrogen bonds of these water molecules by breaking them down. Figure 8 schematically illustrates possible hydrogen bonds around water25 and -45. As shown in the figure, both water molecules neighbor several amino acid residues that are suitable candidates for hydrogen bonding partners. Mutating these amino acid residues may elucidate the nature of the networks of hydrogen bonds.

In contrast to the formation of S390 (Figure 2) and the cysteinyl−flavin adduct (Figure 4), as well as the structural changes of water (Figure 6), the FTIR spectra of amide I vibrations exhibited a marked temperature dependence (Figure 7). At 77−150 K, changes are mostly confined to turn structures (bands at ∼1690 cm^{-1} in Figure 7a), and α-helices change only slightly [peaks at 1660 (+)/1646 (−) cm^{-1} in Figure 7a]. Structural changes at the low temperatures are probably limited to the vicinity of the chromophore, as is the case for rhodopsins (*34*−*36*). Cys966 is located at the joint between the α′A helical and the connected turn structures (Figure 1a). Therefore, the difference IR spectra

[3] While this paper was under review, the structure of *Chlamydomonas* phot-LOV1 was determined (*42*). Interestingly, according to the structure, the reactive cysteine is present in two conformations at ∼100 K. The temperature-dependent reaction of phy3-LOV2 in this study may originate from multiple conformations of the cysteine.

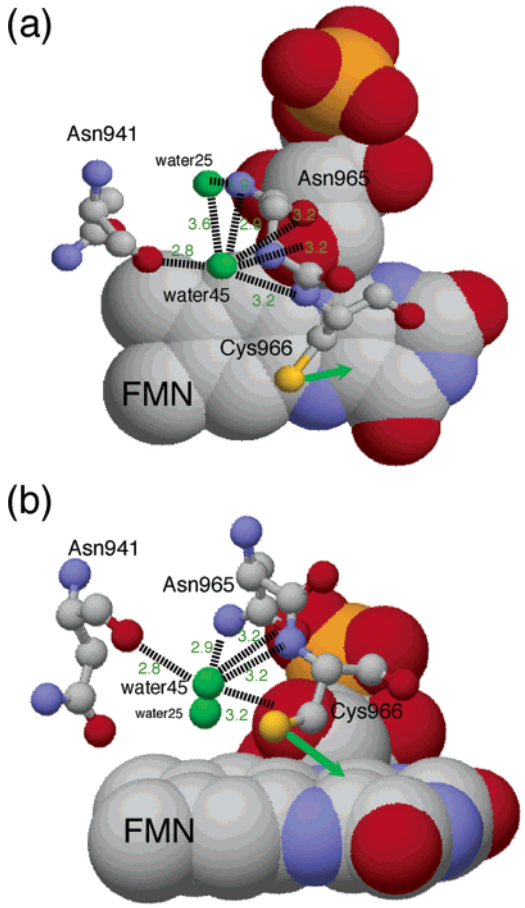

FIGURE 8: Water molecules near FMN. FMN is shown as a space-filling drawing, and the rest is shown as a ball-and-stick drawing. Water molecules are colored green, and the other colors are according to the CPK model. Possible hydrogen bonds are indicated by black dashed lines, the distance of which is shown in angstroms with green numbers. Upon light absorption, the S−H group of Cys966 forms an adduct with FMN at position C(4a) (green arrow). (a) FMN is viewed along the normal to the ring plane. (b) This view is from the bottom of that in panel a.

at 77−150 K may represent the structural changes in this region. Since Asn941 is located in a turn structure between β-strands A and B (Figures 1a and 8), this turn structure could also be varied via the perturbation of these hydrogen-bonded networks. Thus, adduct formation at the low temperatures may alter the local structure around FMN by loosening the hydrogen bonding of turn and α-helical structures as well as breakage of hydrogen bonds of water molecules. At the higher temperatures, the loosening seems to revert (Figure 7b,c) and tightening in the β-structure appears to occur, accompanied by the changes in the helical structure (Figure 7c). It is noted that the phy3-LOV2 construct in this experiment includes the ∼20 and ∼40 extra amino acids upstream and downstream, respectively, of the LOV domain itself. The contribution of these extra amino acids as well as the complex with the kinase domain will be studied in a future.

The temperature-dependent protein changes observed in this study do not necessarily correspond to those in real time. Nevertheless, this observation provides some hints about the stepwise protein structural changes in phy3-LOV2. Light absorption by FMN induces cysteinyl−flavin adduct formation, which perturbs the local structure around FMN. While such perturbation is relaxed, additional changes may take place mainly in β-structure to tighten it, but some occur in the α-helical structure of the protein moiety as well. Interestingly, these changes proceed without any alteration of the shape of UV−visible spectra which is in contrast to the other photoreceptors with isomerizable chromophores. They change their UV−visible spectra along with the sequential formation of multiple intermediates after chromophore isomerization (*12*, *14*). Multiple "S390" states of phy3-LOV2 cannot be distinguished by their UV−visible spectra but have different protein structures, which could be characteristic of photoreceptors having flavin chromophores.

It should be noted that the vibrational bands in the amide I region (1700−1600 cm^{-1}) overlap with those of FMN. In fact, Ataka et al. concluded that most of the light-induced vibrational changes in this region are due to FMN modes in *Chlamydomonas* phot-LOV1, and hence excluded large changes in the protein backbone (*22*). This is in contrast to our interpretation of the data for *Adiantum* phy3-LOV2, and those for oat phot1-LOV2 by Swartz et al. (*17*, *30*). The probable contribution of protein backbone amide I to this region in the latter two samples was shown above by using the 1727 (+)/1710 (−) cm^{-1} bands as a reference for FMN. Recently, it has been proven that LOV2 is essential but that LOV1 is not required for signal tansduction in both *Arabidopsis* phot1 and phot2 (*37*). If protein structural changes are larger in LOV2 than in LOV1 as suggested, they could be correlated with the functional differences between LOV2 and LOV1.

Crosson and Moffat reported that the three-dimensional structure of phy3-LOV2 trapped in the S390 crystal is very similar to that of the unphotolyzed crystal, where slight tilting of the FMN and very small changes in its vicinity are reported (*19*). The authors attempted to explain the signal transduction mechanism without large structural changes in the protein moiety, especially at the protein surface (*19*). In contrast, the FTIR study presented here on phy3-LOV2 proposes progressive alteration of the protein structure without a change in its UV−visible spectrum, which may be involved in the regulation of protein kinase activities in the C-terminal domain connected to the LOV2 domain via a hinge region. We would like to, therefore, emphasize that the light-induced changes in the global protein structure may differ between crystals and solutions as in the case of PYP, another photoreceptive protein of the LOV domain families, where larger changes are observed in solutions than in crystals (*25*−*28*). Analysis of the structural changes in solution, such as by two-dimensional nuclear magnetic resonance spectroscopy, may be required for the understanding of the molecular mechanism of signal transduction.

ACKNOWLEDGMENT

We thank Y. Furutani and Dr. D. Matsuoka for their experimental assistance and Ms. M. Kinoshita for her technical assistance.

REFERENCES

1. Christie, J. M., and Briggs, W. R. (2001) *J. Biol. Chem. 276*, 11457−11460.
2. Liscum, E., and Briggs, W. R. (1995) *Plant Cell 7*, 473−485.
3. Kagawa, T., Sakai, T., Suetsugu, N., Oikawa, K., Ishiguro, S., Kato, T., Tabata, S., Okada, K., and Wada, M. (2001) *Science 291*, 2138−2141.

4. Kinoshita, T., Doi, M., Suetsugu, N., Kagawa, T., Wada, M., and Shimazaki, K. (2001) *Nature 414*, 656−660.
5. Sakai, T., Kagawa, T., Kasahara, M., Swartz, T. E., Christie, J. M., Briggs, W. R., Wada, W., and Okada, K. (2001) *Proc. Natl. Acad. Sci. U.S.A. 98*, 6969−6974.
6. Christie, J. M., Salomon, M., Nozue, K., Wada, M., and Briggs, W. R. (1999) *Proc. Natl. Acad. Sci. U.S.A. 96*, 8779−8783.
7. Kawai, H., Kanegae, T., Christensen, S., Kiyosue, K., Sato, Y., Imaizumi, T., Kadota, A., and Wada, M. (2003) *Nature 421*, 287−290.
8. Huala, E., Oeller, P. W., Liscum, E., Han, I.-S., Larsen, E., and Briggs, W. R. (1997) *Science 278*, 2120−2123.
9. Crosson, S., and Moffat, K. (2001) *Proc. Natl. Acad. Sci. U.S.A. 98*, 2995−3000.
10. Short, T. W., Porst, M., and Briggs, W. R. (1992) *Photochem. Photobiol. 55*, 773−781.
11. Christie, J. M., Reymond, P., Powell, G. K., Bernasconi, P., Raibekas, A. A., Liscum, E., and Briggs, W. R. (1998) *Science 282*, 1698−1701.
12. Kandori, H., Shichida, Y., and Yoshizawa, T. (2001) *Biochemistry (Moscow) 66*, 1197−1209.
13. Andel, F., III, Murphy, J. T., Haas, J. A., McDowell, M. T., van der Hoef, I., Lugtenburg, J., Lagarias, J. C., and Mathies, R. A. (2000) *Biochemistry 39*, 2667−2676.
14. Hellingwerf, K. J., Hendriks, J., and Gensch, T. (2003) *J. Phys. Chem. A 107*, 1082−1094.
15. Salomon, M., Christie, J. M., Knieb, E., Lempert, U., and Briggs, W. R. (2000) *Biochemistry 39*, 9401−9410.
16. Miller, S. M., Massey, V., Ballou, D., Williams, C. H., Jr., Distefano, M. D., Moore, M. J., and Walsh, C. T. (1990) *Biochemistry 29*, 2831−2841.
17. Swartz, T. E., Corchnoy, S. B., Christie, J. M., Lewis, J. W., Szundi, I., Briggs, W. R., and Bogomolni, R. A. (2001) *J. Biol. Chem. 276*, 36493−36500.
18. Salomon, M., Eisenreich, W., Durr, H., Schleicher, E., Knieb, E., Massey, V., Rudiger, W., Muller, F., Bacher, A., and Richter, G. (2001) *Proc. Natl. Acad. Sci. U.S.A. 98*, 12357−12361.
19. Crosson, S., and Moffat, K. (2002) *Plant Cell 14*, 1067−1075.
20. Christopher, W., Kay, M., Schleicher, E., Kuppig, A., Hofner, H., Rudiger, W., Schleicher, M., Fischer, M., Bacher, A., Weber, S., and Richter, G. (2003) *J. Biol. Chem. 278*, 10973−10982.
21. Iwata, T., Tokutomi, S., and Kandori, H. (2002) *J. Am. Chem. Soc. 124*, 11840−11841.
22. Ataka, K., Hegemann, P., and Heberle, J. (2003) *Biophys. J. 84*, 466−474.
23. Ataka, K., Heberle, J., Hehn, D., Dick, B., and Hegemann, P. (2003) *Biophys. J. 84*, 1192−1202.
24. Genick, U. K., Borgstahl, G. E. O., Ng, K., Ren, Z., Pradervand, C., Burke, P. M., Srajer, V., Teng, T.-Y., Schildkamp, W., McRee, D. E., Moffat, K., and Getzoff, E. D. (1997) *Science 275*, 1471−1475.
25. Rubinstenn, G., Vuister, G. W., Mulder, F. A., Dux, P. E., Boelens, R., Hellingwerf, K. J., and Kaptein, R. (1998) *Nat. Struct. Biol. 5*, 568−570.
26. Kandori, H., Iwata, T., Hendriks, J., Maeda, A., and Hellingwerf, K. J. (2000) *Biochemistry 39*, 7902−7909.
27. Xie, A., Kelemen, L., Hendriks, J., White, B. J., Hellingwerf, K. J., and Hoff, W. D. (2001) *Biochemistry 40*, 1510−1517.
28. Imamoto, Y., Kamikubo, H., Harigai, M., Shimizu, N., and Kataoka, M. (2002) *Biochemistry 41*, 13595−13601.
29. Kanegae, T., and Wada, M. (1998) *Mol. Gen. Genet. 259*, 345−353.
30. Swartz, T. E., Wenzel, P., Corchnoy, S. B., Briggs, W. R, and Bogomolni, R. A. (2002) *Biochemistry 41*, 7183−7189.
31. Corchnoy, S. B., Swartz, T. E., Lewis, J. W., Szundi, I., Briggs, W., and Bogomolni, R. A. (2003) *J. Biol. Chem. 278*, 724−731.
32. Kandori, H. (2000) *Biochim. Biophys. Acta 1460*, 177−191.
33. Krimm, S., and Bandekar, J. (1986) *Adv. Protein Chem. 38*, 181−364.
34. Matsui, Y., Sakai, K., Murakami, M., Shiro, Y., Adachi, S., Okumura, H., and Kouyama, T. (2002) *J. Mol. Biol. 324*, 469−481.
35. Schobert, B., Cupp-Vickery, J., Hornak, V., Smith, S. O., and Lanyi, J. K. (2003) *J. Mol. Biol. 321*, 715−726.
36. Edman, K., Royant, A., Nollert, P., Maxwell, C. A., Pebay-Peyroula, E., Navarro, J., Neutze, R., and Landau, E. M. (2002) *Structure 10*, 473−482.
37. Christie, J. M., Swartz, T. E., Bogomolni, R. A., and Briggs, W. R. (2002) *Plant J. 32*, 205−219.
38. Li, H., and Thomas, G. J., Jr. (1991) *J. Am. Chem. Soc. 113*, 456−462.
39. Brown, L. S., Váró, G., Hatanaka, M., Sasaki, J., Kandori, H., Maeda, A., Friedman, N., Sheves, M., Needleman, R., and Lanyi, J. K. (1995) *Biochemistry 34*, 12903−12911.
40. Nishimura, S., Kandori, H., Nakagawa, M., Tsuda, M., and Maeda, A. (1997) *Biochemistry 36*, 864−870.
41. Iwamoto, M., Furutani, Y., Kamo, N., and Kandori, H. (2003) *Biochemistry 42*, 2790−2796.
42. Fedorov, R., Schlichting, I., Hartmann, E., Domratcheva, T., Fuhrmann, M., and Hegemann, P. (2003) *Biophys. J. 84*, 2474−2482.

BI0345135